Conformational preferences of bis(acetonitrile)tetrachloro molybdenum(IV) and tungsten(IV). Crystal structure of $WCl_4(CH_3CN)_2$ and DFT calculations†

Alain Manteghetti,[a] Claude Belin,[a] Monique Tillard-Charbonnel,[a] Jean-Louis Pascal,[a] Eric Clot[b] and Frédéric Favier*[a]

[a] *Laboratoire des Agrégats Moléculaires et Matériaux Inorganiques (CNRS ESA 5072) CC 15, Université Montpellier II, 34095 Montpellier cedex 5, France. E-mail: pasfav@univ-montp2.fr*
[b] *Laboratoire de Structure et Dynamique des Systèmes Moléculaires et Solides (CNRS UMR 5636) Université Montpellier II, 34095 Montpellier cedex 5, France*

Received (in Montpellier, France) 29th July 1998, Accepted 30th November 1998

Crystalline $MoCl_4(NCCH_3)_2$ and $WCl_4(NCCH_3)_2$ have been obtained by an electrocrystallization process and are shown to be isostructural. They crystallize in the monoclinic space group $C2$ with $a = 11.668(3)$, $b = 7.616(5)$, $c = 5.901(2)$ Å, $\beta = 103.04(3)^\circ$ and $a = 11.679(2)$, $b = 7.631(3)$, $c = 5.896(2)$ Å, $\beta = 103.11(2)^\circ$, respectively. The structure of the tungsten compound determined on a single crystal was refined to a final $R(F^2)$ value of 0.046 [$R_w(F^2) = 0.112$] using 745 observed reflections. The metal is in a distorted octahedral environment with 4 chlorine atoms in the equatorial plane and 2 acetonitrile groups in axial positions. DFT optimization of the geometry was done at the B3LYP/LANLD1Z/LANLD2Z/6–31G*/6–31G** and BPW91/LANLD1Z/LANLD2Z/6–31G*/6–31G** levels of theory for singlet and triplet spin states for $WCl_4(NCCH_3)_2$ in *cis* and *trans* conformations, and for $WCl_4(NCCH_3)_x$ ($x = 1$ or 2) with an η^2 coordination of acetonitrile. At the two levels, the energy minimum corresponds to the *trans* structure with a triplet spin state. The electronic spectra were assigned and the vibrational, ^{13}C and ^1H NMR spectroscopies confirm that the previously reported *cis* and η^2 structures are incorrect.

MCl_nL_{y-n} metal complexes with l = tetrahydrofuran, pyridine, $C_nH_{2n+1}CN$, $(C_nH_{2n+1})_2S$, … are often isolated as intermediate products in the synthesis of advanced materials or in a catalytic process, involving a metal chloride moiety dissolved in the corresponding organic solvent. They are also useful precursors for numerous compounds in various applied fields.[1–3] For instance, $ZrCl_4(CH_3CN)_2$ is an intermediate in the synthesis of pure fluorozirconate glasses.[4] Rhenium and molybdenum species of this type have been used for homogeneous olefin and acetylene metathesis[5] and in oxidative chlorination of ketones and aldehydes,[6] respectively.

Depending on the donor ability of the ligand L, MCl_xL_y complexes exhibit a *cis* or *trans* molecular preference.[7–9] These geometries induce some differences in their physical properties and are strongly correlated to the nature and structure of any derived product. Thus, Fowles and later McCarley and their co-workers have shown that, with L = $C_nH_{2n+1}CN$ or $(C_2H_5)_2S$, the magnetic properties of WCl_4L_2 compounds depend on the nature of the ligand L.[10] Using electrochemical techniques, Duff and Heath have extensively investigated ligand additivity in the $RuCl_{6-n}(CH_3CN)_n$ series.[11] In spite of this research, crystallographic data remain scarce.[4,12] Such compounds are generally obtained as microcrystalline or amorphous powders characterized essentially by vibrational spectroscopy.[10,13] Thus, on the basis of IR results, $WCl_4(CH_3CN)_2$ was previously described by Schaeffer-King and McCarley as having a *cis* conformation. More recently, in the course of the synthesis of molybdenum nitride, Kumta and co-workers reported that a part of their transient $MoCl_4(CH_3CN)_x$ ($x = 1$ or 2) was an η^2 (side bound) acetonitrile complex.[14]

We have prepared crystalline $MCl_4(CH_3CN)_2$ compounds (M = Mo and W) by an electrocrystallization process and have determined the crystal structure of $WCl_4(CH_3CN)_2$. The structure of $MCl_4(CH_3CN)_2$ is described in this paper for Mo and W, in which two acetonitrile moieties are in *trans* positions. Other results from X-ray powder diffraction, infrared, Raman, and NMR spectroscopies are also in favor of the *trans* structure. Moreover, DFT calculations have allowed comparison with previously reported structures[10b,14] and confirmed the preference for the *trans* arrangement.

Experimental

$MoCl_5$ and WCl_6 (Aldrich, 99.9 + %) and tellurium (pure, Merck) were used without further purification. CH_3CN (Aldrich, 99%) was dried for several days over molecular sieves (Merck, 4 Å). Bis(acetonitrile)tetrachloro tungsten(IV) and molybdenum(IV) were prepared by electrochemical reduction of WCl_6 and $MoCl_5$ in CH_3CN. A tellurium anode was used and the cell was operated at 300 μA cm^{-2} with a platinum cathode. Crystals were handled in a glove box under dry argon and inserted into thin-walled Lindemann glass capillaries for X-ray diffraction experiments. These two complexes

† *Supplementary material available:* calculated structures and energies of various $WCl_4(\eta^1\text{-}NCCH_3)$ states. Refined positional and thermal parameters for $WCl_4(CH_3CN)_2$. For direct electronic access see http://www.rsc.org/suppdata/nj/1999/165/, otherwise available from BLDSC (No. SUP 57469, 2 pp.) or the RSC Library. See Instructions for Authors, 1999, Issue 1 (http://www.rsc.org/njc).
Non-SI units employed: 1 kcal ≈ 4.18 kJ; 1 eV ≈ 1.6×10^{-19} J; 1 a.u. ≈ 2.63×10^6 J mol^{-1}.

were also prepared by dissolution in acetonitrile of the corresponding chlorides. CH_3CN was distilled under vacuum (1.33 Pa) and solutions were stirred for two days. Acetonitrile was removed under vacuum and $MoCl_4(CH_3CN)_2$ and $WCl_4(CH_3CN)_2$ were quantitatively obtained as dried powders.[10,14]

X-Ray powder diffraction patterns were obtained using Cu-Kα radiation on an automated Philips PW 1965/30 goniometer in the range $10 < 2\theta < 47°$ using a step size of 0.04° and a counting time of 30 s. Powders were held on an aluminium plate protected with a beryllium window (0.025 mm). The lattice parameters of $MoCl_4(CH_3CN)_2$ were calculated using the profile matching option of the FULLPROF program with a pseudo-Voigt peak function.[15] Refined parameters also included a zero point correction, overall scale factor, full width and asymmetry parameters. Common agreement factors are defined as follows $R_{wp} = [\Sigma_w(Y_{obs} - Y_{calc})^2/\Sigma_w Y_{obs}{}^2]^{1/2}$, $R_p = \Sigma(Y_{obs} - Y_{calc})/\Sigma Y_{obs}$.

IR spectroscopic characterization was carried out using a FTIR Bomem DA8 spectrometer, the hygroscopic samples being pressed between silicon plates [(111) cleavage, 1 mm thickness]. Raman spectroscopic data were recorded at room temperature on a Dilor Labram spectrometer using a HeNe laser (632.817 nm, 20 mW) focussed using a BX40 microscope (50x). Sampling was carried out under dry nitrogen into a sealed 5 mm Pyrex tube.

NMR ^{13}C and ^1H spectra were recorded at room temperature in DMSO-d_6 with a Bruker DRX 400. Chemical shifts are related to TMS.

ESR spectra were recorded on a Bruker ER 200D spectrometer with the X band frequency, at room temperature and at 77 K. Samples were sealed in 5 mm diameter quartz tubes and 2,2-di(4-*tert*-octylphenyl)-1-picrylhydrazyl was used as reference.

UV spectra were obtained at room temperature on an UV-visible Cary-3E spectrometer in 2 mm quartz cells using CH_3CN as solvent and reference.

Electrochemical preparation of $WCl_4(CH_3CN)_2$ and $MoCl_4(CH_3CN)_2$

The solution rapidly became dark-purple with the progressive dissolution of WCl_6 in acetonitrile. After a few days of electrolysis, dark-red crystals of $WCl_4(CH_3CN)_2$ appeared in abundance on the Pt electrode.

Reduction of $MoCl_5$ occurred very quickly despite a low electrolysis current, and the resulting brown crystals of $MoCl_4(CH_3CN)_2$ were not suitable for a single crystal X-ray investigation.

Crystallography

Crystal data. $C_4Cl_4H_6N_2W$, $M = 407.76$, $Z = 2$, monoclinic, space group $C2$, $a = 11.679(2)$, $b = 7.631(3)$, $c = 5.896(2)$ Å, $\beta = 103.11(2)°$, $U = 511.77$ Å^3 (by least-squares refinement of the angular positions of 25 reflections automatically centered on the diffractometer, $\lambda = 0.7107$ Å), $Z = 2$, $D_{calc} = 2.646$ Mg m^{-3}, $F(000) = 372$, dark-red plates, crystal dimensions: 0.15 × 0.12 × 0.02 mm.

Data collection and processing. Enraf-Nonius CAD-4 diffractometer, $\omega - (2/3)\theta$ scan mode with a scan width of $1 + 0.35 \tan\theta$, graphite monochromated MoKα radiation; 1608 reflections measured ($2 < \theta < 30°$, octants hkl and $-hkl$). Absorption corrections were made (SHELX 76 numerical procedure,[16a] $\mu_{MoK\alpha} = 128.64$ cm^{-1}, transmission factors range from 0.835 to 0.533). We observed 797 unique averaged reflections ($R_{int} = 0.023$) of which 746 with $I > 3\sigma(I)$ were used in the refinement.

Structure analysis and refinement. The structure was solved in the space group $C2$ with the direct methods provided by SHELXS 86.[16b] The statistical tests indicated a strong preference for a non-centrosymmetric structure. Full-matrix least-squares refinements were carried out using SHELXL 93[16c] in the $C2$ non-centrosymmetric space group. In spite of an increase of the reflection-to-parameter ratio from 14.8 to 23.3 (number of observed reflections/number of parameters varied in the refinement), standard deviations of the positional and thermal parameters in $C2/m$ are of the same order as in $C2$. Futhermore, the refinement in the $C2/m$ centrosymmetric space group leads to R factors and residual electron densities on the final Fourier difference map that are not as good as in the $C2$ space group. Atomic positional and anisotropic thermal parameters for non-hydrogen atoms were refined, and calculated hydrogen positions were included. The weighting scheme $W = 1.0/[\sigma^2(F_o) + (0.074P)^2]$, where $P = (F_o^2 + 2F_c^2)/3$, was applied to all reflections leading to final agreement factors $R(F^2) = 0.046$ and $R_w(F^2) = 0.112$.

CCDC reference number 440/087.

Computational details

All calculations on the complex $WCl_4(CH_3CN)_2$ were done with the GAUSSIAN94 set of programs.[17] Tungsten was represented with the Hay–Wadt relativistic effective core potential (ECP) for the 60 innermost electrons and its associated double-ζ basis set.[18] The chlorine atoms were also described with Los Alamos ECPs and their associated double-ζ basis set[19] augmented by a polarization d function.[20] A 6–31G(d,p) basis set[21] was used for the remaining atoms. Calculations were performed within the framework of density functional theory with two different functionals. The exchange potential was the one proposed by Becke[22a] or its modification including partly the exact Hartree–Fock exchange.[23a] With Becke's exchange, we used the correlation potential of Perdew and Wang[22b] (BPW91) while with the hybrid potential, we used Lee, Yang and Parr's correlation potential[23b] (B3LYP). Several isomers of the complex $WCl_4(CH_3CN)_2$ were optimized. For the *trans* and *cis* isomers both singlet and triplet states were located. For the compounds $WCl_4(\eta^2\text{-}CH_3CN)_x$ ($x = 1$, 2), we searched for local minima on the potential energy surface at the two mentioned levels (B3LYP and BPW91) and for the two spin states ($S = 0$ and $S = 1$). For $x = 1$, only the triplet state converged to a local minimum with both functionals. For $x = 2$, the triplet state could not be optimized and we obtained the *trans*-η^1 compound with both functionals. The compound $WCl_4(\eta^2\text{-}CH_3CN)_2$ was optimized as a local minimum at the B3LYP level as a singlet state. To complete this study, a five-ligand complex, $WCl_4(\eta^1\text{-}CH_3CN)$, was also calculated. The nature of the optimized structure was assigned by numerical calculations of the vibrational frequencies. Potential energy distributions (PED) of vibrational modes were assigned with a home-modified version of the GAR2PED program.[24] Magnetic shielding tensors were calculated at the BPW91 level with the same basis sets as described above. ^{13}C and ^1H NMR chemical shifts (TMS as standard) were calculated with gauge invariant atomic orbitals (GIAO)[25] and continuous set of gauge transformation (CSGT)[26] methods.

Results and discussion

Crystal structure

The molecular structure contains discrete $WCl_4(CH_3CN)_2$ units with acetonitrile groups in the *trans* position (Fig. 1). The tungsten atom is in a distorted octahedral environment as shown by the distances and angles within the chlorine plane: 2 × Cl(1) and 2 × Cl(2) are respectively at 2.351(6) and 2.329(5) Å from W, with a relatively closed Cl(1)—W—Cl(1) angle of 89.0(3)° (Table 1). The nitrogen atoms of the acetoni-

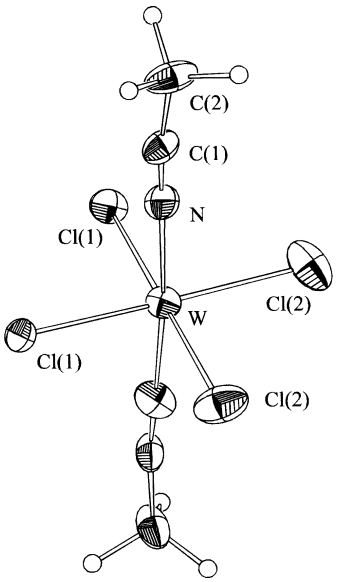

Fig. 1 ORTEP diagram of $WCl_4(CH_3CN)_2$. Thermal ellipsoids are scaled to the 30% probability level.

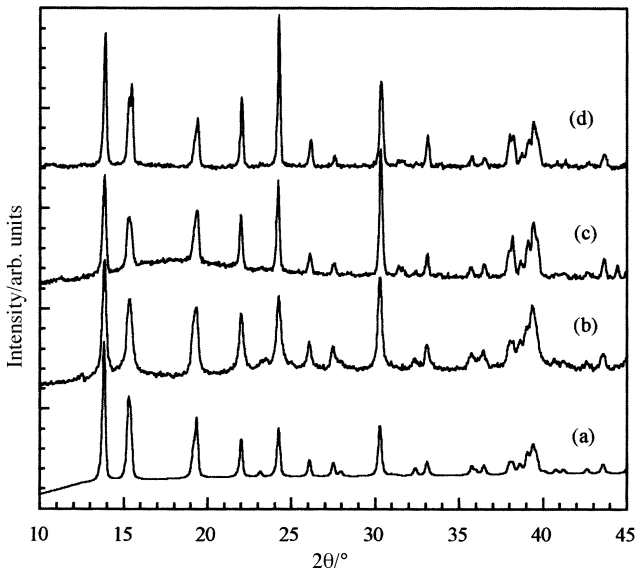

Fig. 2 X-Ray powder diffraction patterns of $MCl_4(CH_3CN)_2$ with M = W (*a*) by electrochemical synthesis (calculated pattern), (*b*) by chemical route, and M = Mo (*c*) by electrochemical synthesis, (*d*) by chemical route.

trile groups are tilted away from the axis [N—W—N = 179(2)°] and the molecule is no longer linear [N—C(1)—C(2) = 170(3)°].

The X-ray powder diffraction pattern of $WCl_4(CH_3CN)_2$ obtained by simple dissolution of the chloride is very close to the pattern calculated using the crystal structure of the electrochemically prepared tungsten compound. Comparison with $MoCl_4(CH_3CN)_2$ (prepared using both synthetic methods) shows that this compound is isostructural with its tungsten homologue (Fig. 2). Lattice parameters of $MoCl_4(CH_3CN)_2$ were refined to $a = 11.668(3)$, $b = 7.616$ (5), $c = 5.901$ (2) Å, $\beta = 103.04$ (3)° with $R_{wp} = 0.088$ and $R_p = 0.104$.

Table 1 Distances (Å) and angles (°) in $WCl_4(CH_3CN)_2$

W—Cl(1)	2.351(6)	C(1)—C(2)	1.49(1)
W—Cl(2)^i	2.329(5)	C(2)—H(1)	1.08
W—N	2.084(8)	C(2)—H(2)	1.08
N—C(1)	1.14(1)	C(2)—H(3)	1.08
Cl(1)—W—Cl(1)^i	89.0(3)	N—C(1)—C(2)	170(3)
Cl(1)—W—Cl(2)	90.6(1)	Cl(2)^i—W—Cl(2)	89.9(2)
N—W—N^i	179(2)	W—N—C(1)	175(2)
Cl(1)—W—N^i	92.1(6)	Cl(1)—W—N	88.9(6)
Cl(2)—W—N^i	88.8(6)	Cl(2)—W—N	90.2(6)

Symmetry code: ^{i} −x, y, −z.

IR spectroscopy and calculations

The IR spectrum of our sample of $WCl_4(CH_3CN)_2$ (Fig. 3) is similar to that reported by Schaeffer-King and McCarley for this compound.[10b] These authors assigned the broad band at about 320 cm^{-1} to νW—Cl modes and on the basis of its multiplicity, concluded that the compound has a *cis* configuration. For such adducts having a C_{2v} *cis* configuration, degenerate modes are split and 4 modes ($2A_1$, B_1, and B_2) are expected. On the other hand, for the *trans* configuration with a local environment around tungsten approximately D_{4h}, only one E_u mode is infrared active. Here, as in the previously reported spectrum, the band at 324 cm^{-1} is very broad and a FTIR measurement at 77 K did not allow separation into its components.

Furthermore, the crystallographic results presented above show that the $MoCl_4(CH_3CN)_2$ complex has the same molecular structure as $WCl_4(CH_3CN)_2$, in which the σ coordination of acetonitrile ligands in a *trans* conformation has been unambiguously demonstrated. Thus, the η^2 coordination of

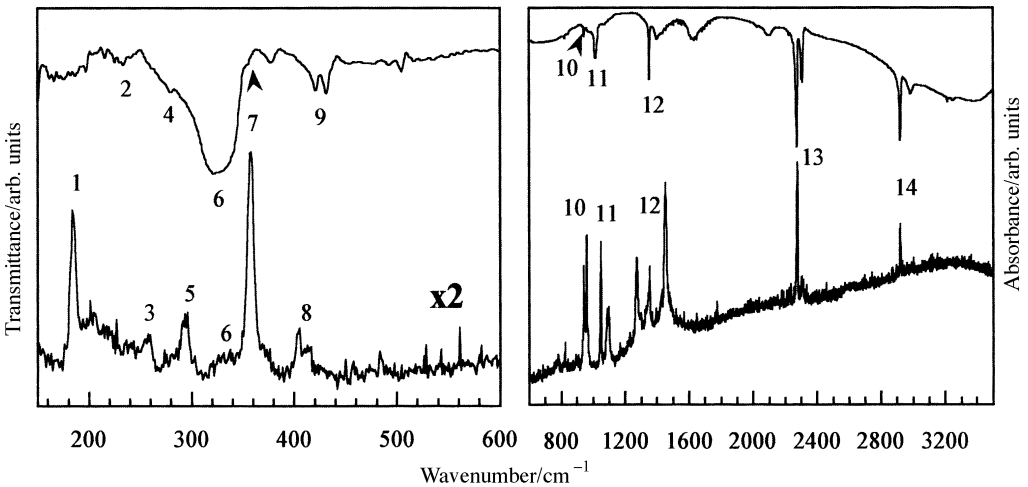

Fig. 3 IR and Raman spectra of *trans*-$WCl_4(CH_3CN)_2$. Numbering is related to data in Table 3. Other assignments: 10 νCC; 11 δCCH + δNCC; 12 δHCH; 13 νNC; 14 νCH.

Table 2 Distances (Å) and angles (°) in experimental and optimized structures of *trans*- and *cis*-$WCl_4(CH_3CN)_2$, $WCl_4(\eta^2\text{-}NCCH_3)$ and $WCl_4(\eta^2\text{-}NCCH_3)_2$

		trans B3LYP		*cis* B3LYP		η^2 coord. B3LYP ($+CH_3CN$)	Bis η^2 coord. B3LYP Singlet	*trans* BPW91		*cis* BPW91		η^2 coord. BPW91 ($+CH_3CN$)
	Expt.	Triplet	Singlet	Triplet	Singlet			Triplet	Singlet	Triplet	Singlet	
W—Cl	2.35–2.38	2.38	2.32–2.43	2.34–2.37	2.30–2.43	2.28–2.44	2.31–2.46	2.37	2.32–2.43	2.34–2.37	2.33–2.41	2.29–2.43
W—N	2.09	2.09	2.07	2.18	2.13	2.08	2.24	2.06	2.04	2.13	2.09	2.04
W—C	—	—	—	—	—	2.25	2.40	—	—	—	—	2.16
N—C	1.13	1.15	1.16	1.16	1.16	1.21	1.19	1.17	1.18	1.17	1.17	1.25
C—C	1.49	1.45	1.45	1.45	1.45	1.47	1.46	1.45	1.45	1.45	1.45	1.47
C—H	1.08	1.09	1.09	1.09	1.09	1.09	1.09	1.10	1.10	1.10	1.10	1.10
Cl—W—Cl	88.2–90.6	89.9–90.1	89.6–90.4	91.2–99.0	90.4	85.5–88.4	90.0	89.9–90.1	90.0	90.5–98.1	99.1	85.2–87.2
N—W—N	175.6	179.7	178.9	98.0	75.2	—	—	179.9	180.0	97.06	85.6	—
Cl—W—N	87.0–92.1	89.8–90.1	89.5–90.5	81.5–85.4	85.9–89.4	84.6–117.9	90.0–104.9	89.9–90.1	89.9–90.0	82.4–86.2	81.5–85.6	86.1–114.9
W—N—C	175.0	179.6	179.2	180.9	174.8	81.5	83.6	179.8	179.9	174.9	177.8	78.1
N—C—C	175.2	179.7	179.9	179.3	180.0	150.7	—	179.9	179.7	178.9	179.3	146.2
E/a.u.	—	−393.369613	−393.336848	−393.361003	−393.319489	−393.282990	−393.283276	−393.462987	−393.433914	−393.452045	−343.408650	−393.387016

Corresponding energies are also given.

$NCCH_3$ proposed by Kumta and co-workers[14] for $MoCl_4(CH_3CN)_x$ ($x = 1$ or 2) seems doubtful in the solid state. In fact, this description is based only on the assignment of an IR band at 1680 cm^{-1} to a disturbed stretching mode of the CN bond involved in an η^2 coordination. Noteworthy is the fact that these compounds are hygroscopic and the alternative assignment of this band, which progressively increase with time, to δOH of undesirable water cannot be excluded (no particular precautions taken in sample preparation). Since the νOH domain was omitted in their spectrum it is difficult to reach a firm conclusion at this stage.

In an attempt to explain the discrepancy between the *cis* conformation proposed by McCarley and colleagues, the η^2 coordination of CH_3CN proposed by Kumta and co-workers and our *trans* configuration, we have optimized these various structures within the framework of density functional theory (DFT). Although these energy values (Table 2) correspond to isolated gaseous molecules at 0 K, we can discuss their relative stabilities. In all cases (B3LYP or BPW91), (*i*) the *trans* configuration is more stable in a triplet than in singlet spin state [$\Delta E_{B3LYP} = (E_{sing} - E_{trip})_{B3LYP} = 20.8$ kcal $mol^{-1} = 0.9$ eV and $\Delta E_{BPW91} = (E_{sing} - E_{trip})_{BPW91} = 18.3$ kcal $mol^{-1} = 0.8$ eV], so in the following discussion, only the triplet state will be considered; (*ii*) the energetic difference between *cis* and *trans* conformations (both in triplet state) is slight ($\Delta E_{B3LYP} =$ 4.6 kcal $mol^{-1} = 0.2$ eV and $\Delta E_{BPW91} = 6.9$ kcal $mol^{-1} = 0.3$ eV) and the crystallization of the *trans* conformation is essentially driven by the crystal packing energy; (*iii*) the η^2 coordination of acetonitrile ligand in $WCl_4(\eta^2\text{-}CH_3CN)$, as well as in $WCl_4(\eta^2\text{-}CH_3CN)_2$, is significantly less favorable {$[(E_{WCl_4(\eta^2\text{-}CH_3CN)} + E_{CH_3CN}) - E_{trans}]_{B3LYP} = 54.3$ kcal $mol^{-1} = 2.4$ eV and $\Delta E_{B3LYP} = (E_{WCl_4(\eta^2\text{-}CH_3CN)_2} - E_{trans} = 33.6$ kcal $mol^{-1} = 1.5$ eV}. Since there is a convergence to stable stationary points, these conformations can be envisaged as transient states in solution even though they are high in energy; (*iv*) for the five-ligand complex with acetonitrile in an η^1 coordination mode, the system $WCl_4(\eta^1\text{-}CH_3CN) + CH_3CN$, is globally more than 20 kcal mol^{-1} (0.9 eV) higher in energy than corresponding *trans* or *cis* adducts (see supplementary material).

Optimized *trans* geometries are close to that of the experimental structure (Table 1). For the *cis* and η^2 complexes, distances and angles are consistent with data previously reported.[27–30] The structural descriptions given by Schaffer-King and McCarley as well as by Kumta and co-workers are based on infrared data analysis and since selection rules give contradictory results, calculated frequencies could help to assign the vibrational spectra of the three adducts. The calculated frequencies and relative intensities (Table 3) are overall in good agreement with those of the experimental spectra confirming the consistency of our optimized structures. In the mid-frequency range above 500 cm^{-1}, there are no differences between the spectra of *trans*- and *cis*-$WCl_4(CH_3CN)_2$ complexes. Owing to the low coupling of characteristic vibrations of CH_3CN ligand with those of the WCl_4N_2 octahedral core, this frequency region does not allow distinction between the *trans* or *cis* σ-coordination mode of acetonitrile. Below 500 cm^{-1}, differences in frequencies as well as in intensities are more marked, especially around 320 cm^{-1}.

For *trans*-$WCl_4(CH_3CN)_2$, the experimental band at 324 cm^{-1}, strong and broad, is essentially composed of two νW—Cl modes at about 319 cm^{-1} (Table 3, unscaled BPW91). These modes can be assigned to a degenerate E_u mode (D_{4h} pseudo-octahedral symmetry around tungsten). A

Table 3 Experimental and unscaled calculated vibrational frequencies for *trans*-$WCl_4(CH_3CN)_2$. Calculated vibrational frequencies for *cis*-$WCl_4(CH_3CN)_2$ and $WCl_4(\eta^2\text{-}CH_3CN)$ are also given

	trans-$WCl_4(CH_3CN)_2$ (150–450 cm^{-1} range)				
	Expt.				
	IR[a]	Raman[b]	B3LYP[c] Triplet	BPW91[c] Triplet	PED[d]
ν_1	—	186(40)	196(6.6)	188(0.0)	70% δNWCl + 30% δNCC
ν_2	233(w)	—	226(0.1)	227(1.0)	60% δNWCl + 40% δNCC
ν_3	—	256(5)	268(9.1)	264(7.5)	100% νWN
ν_4	280(sh)	—	275(0.0)	279(0.0)	100% νWCl
ν_5	—	294(15)	288(0.0)	293(0.0)	100% νWN
ν_6	324(vs)	—	311(106.2)	318(107.5)	60% νWCl + 20% δNCC + 20% NC torsion
			331(119.3)	319(107.5)	} 100% νWCl
ν_7	354(sh)	356(60)	334(0.2)	332(0.0)	
ν_8	—	403(10)	401(0.0)	387(0.0)	50% δNCC + 30% δWNC + 20% δNWCl
		409(10)			} 50% δNCC + 50% NC torsion
ν_9	426(m)	—	425(1.7)	427(1.2)	
	432(m)		434(1.9)		40% δNWCl + 30% δNCC + 25% δWNC
cis-$WCl_4(CH_3CN)_2$ (characteristic frequencies in the 300–350 cm^{-1} range)					
	B3LYP (triplet)[c]		BPW91 (triplet)[c]		
ν_1	312(74.8)		310(51.1)		} 100% νWCl
ν_2	319(13.9)		316(7.9)		
ν_3	325(101.4)		321(88.7)		
ν_4	353(48.3)		349(45.7)		
$WCl_4(\eta^2\text{-}CH_3CN)$ (characteristic frequencies of WCl and $\eta^2\text{-}CH_3CN$)					
	B3LYP[c]		BPW91[c]		
ν_1	308(19.9)		319(58.0)		} 90% νWCl + 5% δCWCl + 5% δNWCl
ν_2	326(74.3)		367(11.5)		
ν_4	384(68.0)		395(5.7)		
ν_5	544(90.9)		558 (75.1)		40% νWN + 10% νWC + 30% δNCC + 10% δNWCl + 10% δCWCl
ν_6	1959(31.6)		1802(24.5)		90% νNC + 10% νCC

[a] Intensities are given as follows: sh, shoulder; w, weak; m, medium; s, strong; vs, very strong. [b] Relative intensities are given as a percentage. [c] Calculated IR intensity (arb. units) in parentheses follows wavenumber (cm^{-1}). [d] Potential energy distributions (PED) are given as percentages.

weak coupling of one of the components of the E_u mode with δN—C—C and C—C torsions causes the slight loss of degeneracy (less than 1 cm^{-1}). The multiplicity and position of the other bands are well reproduced by the calculations.

The experimental spectrum of *trans*-$WCl_4(CH_3CN)_2$ shows some marked differences with respect to the calculated spectrum of *cis*-$WCl_4(CH_3CN)_2$. The 300–350 cm^{-1} range is described by 4 νW—Cl bands [310, 316, 321, and 349 cm^{-1} with BPW91 and 312, 319, 325, and 353 cm^{-1} with B3LYP (Table 3)], which nevertheless reasonably agrees with the experimental spectrum of the *trans* complex in this domain.

An analysis based only on the 320 cm^{-1} broad band led to an unsatisfactory description of the structure. Anyway, in this case, vibrational spectroscopy does not allow a discrimination to be made between the *cis* or *trans* coordination modes of the two acetonitrile units.

For $WCl_4(\eta^2\text{-}CH_3CN)$ as well as for $WCl_4(\eta^2\text{-}CH_3CN)_2$, νW—Cl bands are located in the 300–400 cm^{-1} range. Their intensity distribution and multiplicity are close to those of *cis* $WCl_4(CH_3CN)_2$. Among the remaining intense bands of $WCl_4(\eta^2\text{-}CH_3CN)$, two of them exclusively correspond to the NC molecular fragment in interaction with the tungsten: a band at 536 cm^{-1} (BPW91 scaled by 0.96) assigned to W—N stretching (50%) and to δN—C—C (30%) (plus 10% for νW—C), and at 1729 cm^{-1} (BPW91 scaled by 0.96), a band 80% composed of νN—C weakly coupled with νC—C (10%). For $WCl_4(\eta^2\text{-}CH_3CN)_2$, the νNC band is calculated to be at 2032 cm^{-1} (B3LYP scaled by 0.96). Kunta and colleagues assigned a band at 1680 cm^{-1} in the IR spectrum of a solution of $MoCl_5$ in acetonitrile to a disturbed νNC vibration. This band is, however, located in the same IR domain as the δOH deformation mode of water, which can sometimes be broad. The band at 536 cm^{-1}, outside any OH vibration domain, is better used to unambiguously characterize an η^2 coordination of acetonitrile. A band at 1680 cm^{-1} is, in any case, too low in frequency to be assigned to a stretching vibration of a perturbed N=C in η^2 coordination. The calculated value of this band at 1729 cm^{-1} is close to those previously reported at 1725[27] and at 1750 cm^{-1} for parent complexes.[28] Kunta and co-workers argued their assignment on the basis of these same references. IR spectroscopy alone does not allow a firm conclusion to be reached, and ^1H and ^{13}C NMR in solution are known to give more reliable results for the determination of the coordination mode of an organic ligand such as acetonitrile.

^1H and ^{13}C NMR spectroscopy

Experimental ^1H and ^{13}C spectra of our *trans* $WCl_4(CH_3CN)_2$ in DMSO-d_6 consist of single peaks at 2.07 ppm and at 2.05 and 118.96 ppm, respectively. Our calculations with CSGT and GIAO methods of the ^{13}C chemical shifts are in good agreement, especially for the position of the cyano carbon calculated to be at 119 and 114 ppm, respectively. The chemical shift is very sensitive to the environment of acetonitrile and is a reliable probe for the coordination mode of this ligand. The calculated corresponding chemical shift at 115–120 ppm for the *trans* complex increases to about 140 ppm for a *cis* complex and to 207 ppm for an η^2 coordination. No NMR lines are observed above 120 ppm in our experimental ^{13}C spectrum, confirming that the *trans* conformation of $WCl_4(CH_3CN)_2$ is retained even in solution.

ESR spectroscopy

At 298 and 77 K, ESR spectra of the molybdenum and tungsten complexes exhibit a single resonance without hyperfine structure (with $\Delta H = 75$ and 150 G, respectively). Spectra of 6.5×10^{-2} (error 10%) paramagnetic sites Mo^V per molybdenum atom can be modeled with the usual values of $g_{\|} = 1.940$ and $g_{\perp} = 1.956$.[31] At 77 K, the spectrum of the tungsten complex corresponds to 5×10^{-3} sites per tungsten atom and gives $g_{\|} = 1.700$ and $g_{\perp} = 1.778$. These low values of g are close to those previously reported for WX_4L_2 complexes[10], for silicate and phosphate W^V glasses[32] or oxotungstate(v) complexes.[33] At room temperature, this signal is shifted to higher field with $g_{\|} = 2.207$ and $g_{\perp} = 2.277$. These spectra are characteristic of paramagnetic Mo^V and W^V impurities in a quasi-axial environment.

UV spectroscopy

In the spectrochemical series, chlorine and acetonitrile ligands are close enough to consider that $MCl_4(CH_3CN)_2$ (M = Mo, W) complexes display a pseudo-octahedral geometry.[34] Spectral analysis is therefore made using the Tanabe–Sugano splitting diagram in pseudo-octahedral geometry. For a transition metal d^2 ion in such an environment, three d–d transitions are expected from the $^3T_{1g}$ ground term: $^3T_{1g} \rightarrow {}^3T_{2g}$ (I), $^3T_{1g} \rightarrow {}^3A_{2g}$ (II) and $^3T_{1g} \rightarrow {}^3T_{1g}$ (III). The second transition (II) is a two-electron transition and thus, is normally very weak, depending on the *Dq* and *B* parameters, it can become higher in energy than $^3T_{1g} \rightarrow {}^3T_{1g}$. The spectrum of $MoCl_4(CH_3CN)_2$ shows two d–d transitions, whereas the more intense charge transfer (CT) ligand-to-metal transition occurs below 250 nm (40 000 cm^{-1}). The two low bands are close in energy; they can be assigned to transitions I (λ_{max} = 365 nm, $\varepsilon = 4700$ L m^{-1} mol^{-1}) and III ($\lambda_{max} = 312$ nm, $\varepsilon = 34300$ L m^{-1} mol^{-1}) of a d^2 ion.[34] As for $MoCl_6^{2-}$ ion,[35] its spectrum gives a high value of Dq/B. At low concentration in CH_3CN solvent, the spectrum of $WCl_4(CH_3CN)_2$ can be unambiguously deconvoluted in three bands corresponding respectively to $^3T_{1g} \rightarrow {}^3T_{2g}$ ($\lambda_{max} = 315$ nm, $\varepsilon = 14500$ L m^{-1} mol^{-1}), CT ($\lambda_{max} = 267$ nm, $\varepsilon = 85200$ L m^{-1} mol^{-1}) and $^3T_{1g} \rightarrow {}^3T_{1g}$ transitions ($\lambda_{max} = 241$ nm, $\varepsilon = 27250$ L m^{-1} mol^{-1}). Energetic inversion of d–d transitions and CT often occurs for heavy metals in high oxidation states.[36] According to its *Dq* and *B* values, the $^3T_{1g} \rightarrow {}^3A_{2g}$ transition should occur at 154 nm (65 000 cm^{-1}), too high in energy to be observed in this experiment.

Conclusion

$MCl_4(CH_3CN)_2$ (M = Mo or W) display a *trans* conformation of the acetonitrile groups. DFT calculations demonstrate that *cis* and *trans* conformations cannot in this case be distinguished using IR and Raman spectroscopies. ^{13}C and ^1H NMR spectroscopies are more sensitive tools for the various conformations. DFT calculations also show that an η^2 coordination of acetonitrile in such compounds is unlikely, even in solution.

Acknowledgements

We thank R. Astier for operating the Nonius CAD-4 and B. Deroide for ESR measurements. The Centre National Universitaire Sud de Calcul (CNUSC) is gratefully acknowledged for computational facilities.

References

1 (*a*) E. L. Manzer, *Inorg. Synth.*, 1982, **21**, 135; (*b*) M. W. Anker, J. Chatt, G. J. Leigh and A. G. Wedd, *J. Chem. Soc., Dalton Trans.*, 1975, 2639.
2 A. Van Den Bergen, K. S. Murray and B. O. West, *Aust. J. Chem.*, 1972, **25**, 705.
3 C. Kan, *J. Chem. Soc., Dalton Trans.*, 1982, 2309.
4 J. Guery, M. Leblanc and C. Jacoboni, *Eur. J. Solid State Inorg. Chem.*, 1989, **26**, 289.

5 I. M. Gardiner, M. A. Bruck, P. A. Wexler and D. E. Wigley, *Inorg. Chem.*, 1989, **28**, 3688.
6 S. Roh and J. W. Bruno, *Inorg. Chem.*, 1986, **25**, 3105.
7 E. Turin, R. M. Nielson and A. E. Merbach, *Inorg. Chim. Acta*, 1987, **134**, 67.
8 (*a*) G. N. Dolenko, O. Kh. Poleshchuk, V. P. Elin, A. L. Litvin, I. V. Udachin and A. L. Ivanovskii, *Izv. Akad. Nauk. SSSR, Ser. Khim.*, 1989, **11**, 2522; (*b*) M. Mitsuo and O. Tsutomi, *Bull. Chem. Soc. Jpn.*, 1990, **63**, 1206.
9 (*a*) R. D. Willet and R. E. Rundle, *J. Chem. Phys.*, 1964, **40**, 838; (*b*) J. Fernandez Bertran and E. Reguera Ruiz, *Spectrochim. Acta, Part A*, 1993, **49**, 43.
10 (*a*) E. A. Allen, B. J. Brisdon and G. W. A. Fowles, *J. Chem. Soc.*, 1964, 4531; (*b*) M. A. Schaeffer-King and R. E. McCarley, *Inorg. Chem.*, 1973, **12**, 1972.
11 C. M. Duff and G. A. Heath, *Inorg. Chem.*, 1991, **30**, 2528.
12 (*a*) D. Fenske and G. Baum, *Z. Naturforsch., Teil B*, 1990, **45**, 1210; (*b*) S. I. Troyanov and G. N. Mazo, *Moscow Univ. Chem. Bull.*, 1984, **39**, 606; (*c*) M. Webster and H. E. Blayden, *J. Chem. Soc.*, 1969, A2443.
13 (*a*) C. Dubois, *Bull. Soc. Chim. Fr.*, 1978, 143; (*b*) Y. Kawano, Y. Hase and O. Sala, *J. Mol. Struct.*, 1976, **30**, 45.
14 M. A. Sriram, P. N. Kumta and E. I. Ko, *Chem. Mater.*, 1995, **7**, 859.
15 J. Rodriguez-Carvajal, *FULLPROF*, *in Collected Abstracts of Powder Diffraction Meeting*, Toulouse, France, 1990, p. 127.
16 (*a*) G. M. Sheldrick, *SHELX 76*, *Program for Crystal Structure Determinations*, University of Cambridge, Cambridge, 1976; (*b*) G. M. Sheldrick, *SHELXS* 86, *Program for Crystal Structure Solution*, University of Göttingen, Göttingen, 1986; (*c*) G. M. Sheldrick, *SHELXL 93*, *Program for Crystal Structure Refinements*, University of Göttigen, Göttingen, 1993.
17 M. J. Frisch, G. W. Trucks, H. B. Schelgel, P. M. W. Gill, B. G. Johnson, M. A. Robb, J. R. Cheeseman, T. Keith, G. A. Petersson, J. A. Montgomery, K. Raghavachari, M. A. Al-Laham, V. G. Zakrewski, J. V. Ortiz, J. B. Foresman, J. Ciolowski, B. B. Stephanov, A. Nanayakkara, M. Challacombe, C. Y. Peng, P. Y. Ayala, W. Chen, M. W. Wong, J. L. Andres, E. S. Replogle, R. Gomperts, R. L. Martin, D. J. Fox, J. S. Binkley, D. J. Defrees, J. Baker, J. P. Stewart, M. Head-Gordon, C. Gonzalez and J. A. Pople, *GAUSSIAN 94*, *Rev. B3*, Gaussian, Inc., Pittsburgh, PA, 1995.
18 P. J. Hay and W. R. Wadt, *J. Chem. Phys.*, 1985, **82**, 299.
19 W. R. Wadt and P. J. Hay, *J. Chem. Phys.*, 1985, **82**, 284.
20 A. Höllwarth, M. Böhme, S. Dapprich, A. W. Ehlers, A. Gobbi, V. Jonas, K. Köhler, R. Stegmann, A. Veldkamp and G. Frenking, *Chem. Phys. Lett.*, 1993, **208**, 237.
21 P. C. Harchaman and J. Pople, *J. Theor. Chem. Acta*, 1973, **28**, 213.
22 (*a*) A. D. Becke, *Phys. Rev. A*, 1988, **38**, 3098; (*b*) J. P. Perdew and Y. Wang, *Phys. Rev. B*, 1992, **45**, 13244.
23 (*a*) A. D. Becke, *J. Chem. Phys.*, 1993, **98**, 5648; (*b*) C. Lee, W. Yang, and R. G. Parr, *Phys. Rev. B*, 1988, **37**, 785.
24 J. M. L. Martin and C. Van Alsenoy, *GAR2PED*, Antwerp University, Antwerp, 1995.
25 K. Wolinski, J. F. Hinton and P. Pulay, *J. Am. Chem. Soc.*, 1990, **112**, 8251.
26 T. A. Keith and F. W. Bader, *Chem. Phys. Lett.*, 1993, **210**, 223
27 R. M. Bullock, C. E. L. Headford, S. E. Kegley and J. R. Norton, *J. Am. Chem. Soc.*, 1985, **107**, 727.
28 T. C. Wright, G. Wilkinson, M. Motevalli and M. B. Hursthouse, *J. Chem. Soc., Dalton Trans.*, 1986, 2017.
29 H. Junicke, K. Schenzel, F. W. Heinemann, K. Pelz, H. Bögel and D. Steinborn, *Z. Anorg. Allg. Chem.*, 1997, **623**, 603.
30 D. Fenske, G. Baum, H. W. Swidersky, and K. Denicke, *Z. Naturforsch., Teil B*, 1990, **45**, 1210.
31 B. Deroide, P. Belougne and J. V. Zanchetta, *J. Phys. Chem. Solids*, 1987, **42**, 1197.
32 N. R. Yafaev, N. S. Garif' Yanov and Yu. V. Yablokov, *Sov. Phys. Sol.*, 1963, **5**, 1216.
33 H. Kon and N. E. Sharpless, *J. Phys. Chem.*, 1966, **70**, 105.
34 A. B. P. Lever, *Inorganic Electronic Spectroscopy*, Elsevier, Amsterdam, 2nd edn., 1984, p. 407.
35 S. M. Horner and S. Y. Tyree, Jr., *Inorg. Chem.*, 1964, **2**, 568.
36 A. B. P. Lever, *Inorganic Electronic Spectroscopy*, Elsevier, Amsterdam, 2nd edn., 1984, p. 329.

Paper 8/05973J